Synthesis, Structure, and Properties of Two New Ruddlesden−Popper Phase Analogues of SFMO (Sr_2FeMoO_6)

Falak Sher,[†,‡] A. J. Williams,[‡] A. Venimadhev,[§] Mark G. Blamire,[§] and J. Paul Attfield*[,‡]

Department of Chemistry, University of Cambridge, Lensfield Road, Cambridge, CB2 1EW, U.K., Centre for Science at Extreme Conditions, University of Edinburgh, King's Buildings, Mayfield Road, Edinburgh, EH9 3JZ, U.K., and Department of Materials Science and Metallurgy, University of Cambridge, Pembroke Street, Cambridge, CB2 3QZ, U.K.

Received November 30, 2004

The substitutional chemistry and magnetoresistive properties of SFMO (Sr_2FeMoO_6) have been extensively studied in recent years. We report two new analogue Ruddlesden−Popper phases of SFMO: Sr_3FeMoO_7 and Sr_4FeMoO_8. Both phases have a tetragonal structure (*I*4/*mmm*) with no Fe/Mo cation order. Neutron diffraction data suggest that there is no long-range spin order in Sr_3FeMoO_7, whereas antiferromagnetic order is evidenced for Sr_4FeMoO_8. Both materials show ferromagnetic hysteresis loops at 5 K with saturated moments of 0.8 μ_B and 0.2 μ_B for Sr_3FeMoO_7 and Sr_4FeMoO_8, respectively. Resistivity measurements show these materials to be semiconducting with band gaps of 125 and 46 meV for Sr_4FeMoO_8 and Sr_3FeMoO_7, respectively. No magnetoresistance effect was observed for either of the materials.

Introduction

Recently there has been a tremendous amount of interest in materials exhibiting a colossal magnetoresistance (CMR) effect, due to their potential applications in spintronic devices.[1] Of particular interest are the manganese based perovskites, $AMnO_3$,[2] and the double perovskite Sr_2FeMoO_6 (SFMO).[3] Following the observation of CMR effect in $Sr_{1.8}La_{1.2}Mn_2O_7$,[4] research was extended into the magnetotransport properties of layered Ruddlesden−Popper (RP)[5] phases of the general formula $A_{n+1}B_nO_{3n+1}$ as well. The RP compounds consist of $A_nB_nO_{3n}$ perovskite-like blocks, *n* octahedra thick, separated by a rock-salt like layer of the composition AO (Figure 1).

A large number of transition metals can occupy the B-cation site within the oxide octahedra and the electronic properties are very sensitive to the chemical composition.[6] For example, Sr_2RuO_4 ($n = 1$) is a spin-triplet p-wave superconductor,[7,8] whereas the isostructural analogue Sr_2MoO_4[9] shows metallic behavior but does not show superconductivity down to 30 mK, and Sr_2FeO_4 is a Mott-type antiferromagnetic semiconductor with a Neel temperature $T_N = 60$ K.[10] Similarly, $Sr_3Fe_2O_{7-\delta}$ is a semiconductor that orders antiferromagnetically at low temperatures for the whole range of oxygen nonstoichiometry and also suffers charge disproportionation.[11] $Sr_3Mn_2O_7$ is an antiferromagnetic insulator with $T_N = 160$ K[12] but a substitution of La^{3+} for Sr^{2+} in $Sr_{1.8}La_{1.2}Mn_2O_7$[4] results in mixed valence Mn^{3+}/Mn^{4+} ions, and hence a strong ferromagnetic interaction, which arises from the double-exchange mechanism[13,14] between

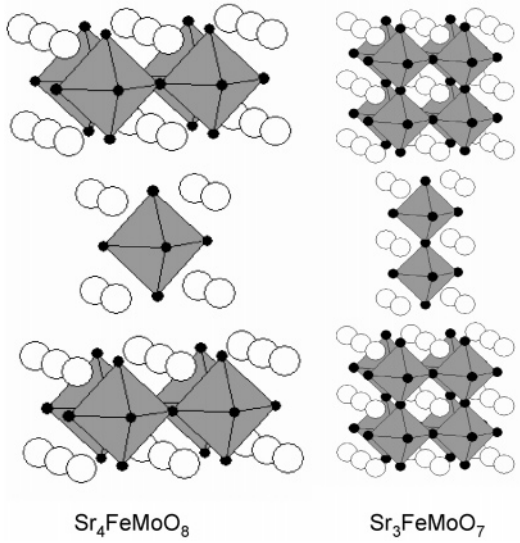

Figure 1. Crystal structures of Sr_3FeMoO_7 and Sr_4FeMoO_8. Fe/MoO_6 octahedra are shaded, whereas Sr atoms are drawn as circles.

* To whom correspondence should be addressed. E-mail: j.p.attfield@ed.ac.uk. Tel: +44 131 651 7229. Fax: +44 131 650 4743.
† Department of Chemistry, University of Cambridge.
‡ University of Edinburgh.
§ Department of Materials Science and Metallurgy, University of Cambridge.

(1) Coey, J. M. D.; Chien, C. L. *MRS Bull.* **2003**, *28*, 724.
(2) Ramirez, A. P. *J. Phys.: Condens. Matter* **1997**, *9*, 8171.
(3) Kobayashi, K.-I.; Kimura, T.; Sawada, H.; Terakura, K.; Tokura, Y. *Nature* **1998**, *395*, 677.
(4) Moritomo, Y.; Asamitsu, A.; Kuwahara, H.; Tokura, Y. *Nature* **1996**, *380*, 141.
(5) Ruddlesden, S. R.; Popper, P. *Acta Crystallogr.* **1958**, *11*, 54.
(6) Battle, P. D.; Rosseinsky, M. J. *Curr. Opin. Solid State Mater. Sci.* **1999**, *4*, 163.
(7) Ishida, K.; Mukuda, H.; Kitaoka, Y.; Asayama, K.; Mao, Z. Q.; Mori, Y.; Maeno, Y. *Nature* **1998**, *396*, 658.
(8) Luke, G. M.; Fudamoto, Y.; Kojima, K. M.; Larkin, M. I.; Merrin, J.; Nachumi, B.; Uemura, Y. J.; Maeno, Y.; Mao, Z. Q.; Mori, Y.; Nakamura, H.; Sigrist, M. *Nature* **1998**, *394*, 558.
(9) Shirakawa, N.; Ikeda, S. I. *Physica C* **2001**, *364*−*365*, 309.
(10) Adler, P. *J. Solid State Chem.* **1994**, *108*, 275.
(11) Adler, P. *J. Solid State Chem.* **1997**, *130*, 129.
(12) Mitchel, J. F.; Millburn, J. E.; Medarde, M.; Short, S.; Jorgensen, J. D.; Fernandez-Diaz, M. T. *J. Solid State Chem.* **1998**, *141*, 599.
(13) Zener, C. *Phys. Rev.* **1951**, *82*, 403.

10.1021/cm0479178 CCC: $30.25
Published on Web 03/09/2005

Mn^{3+} and Mn^{4+}. There are also examples of RP compounds in which the B site has been partially occupied by other transition metal ions. It has been reported that the partial substitution of Fe by Co increases both the conductivity and the ferromagnetic interactions in $Sr_3Fe_{2-x}Co_xO_{7-\delta}$ compounds[15] and a large MR effect has been reported in $Sr_3FeCoO_{7-\delta}$ at 10 K.[16] Both Sr_3FeRuO_7 and Sr_4FeRuO_8 show a spin glass-type behavior.[17] Similarly, a spin glass behavior and magnetoresistance of 8%, in 14 T field, has been reported in both Sr_3MnRuO_7 and $Sr_2Mn_{0.5}Ru_{0.5}O_4$ compounds.[18]

In view of the fact that both simple and layered manganese perovskites show a large MR effect, it is worthwhile to explore the SFMO analogue RP phases in a search for new CMR materials. Here we report the synthesis, crystal structure, and magnetic and electrical properties of two new RP phases, Sr_3FeMoO_7 and Sr_4FeMoO_8.

Experimental Details

Polycrystalline samples of Sr_3FeMoO_7 and Sr_4FeMoO_8 were prepared by conventional solid-state reaction. Stoichiometric amounts of $SrCO_3$, Fe_2O_3, and MoO_3 were mixed, ground, pressed into pellets, and calcined at 900 °C for 8 h in air. The calcined mixtures were reground, pressed, and sintered twice at 1100 °C for 8 h under flowing 5% H_2/95% Ar in a tube furnace.

Phase purity of the samples was checked using a Bruker D8 Advance X-ray diffractometer (Cu Kα radiation, $\lambda = 1.5406$ Å). Neutron diffraction data were collected on the high-resolution powder diffractometer (HRPD) at the ISIS Facility, United Kingdom for both samples at 2 and 300 K, using collection times of approximately 3 h at each temperature. Profiles from the backscattering ($2\theta = 168°$) and the $2\theta = 90°$ detector banks were Rietveld analyzed using the general structural analysis system (GSAS) program.[19] Magnetic susceptibility measurements were performed using a Quantum Design SQUID magnetometer. The dc molar susceptibility of each sample was measured over the temperature range $5 \leq T/K \leq 300$ in an applied field of 100 Oe. The field dependence of the magnetization was studied over the range $-50 \leq H/kOe \leq 50$ at 5 K. Resistivity measurements were made in zero and in a 50 kOe field, using a standard four-probe geometry, on a Quantum Design physical properties measurement system (PPMS).

Results and Discussion

Structural Characterization. The X-ray powder diffraction patterns of both Sr_4FeMoO_8 and Sr_3FeMoO_7 were indexed in a body-centered tetragonal space group *I*4/*mmm* (Figure 2), consistent with previous studies on analogous Ruddlesden−Popper materials.[16−18] Neutron diffraction data for Sr_4FeMoO_8, collected at 300 and 2 K, were Rietveld analyzed. The resulting structural parameters and atomic coordinates are presented in Table 1 and the corresponding bond lengths are listed in Table 2. The observed and calculated diffraction profiles are plotted in Figure 3. Small impurity phases (<3 wt %) of $Sr_3Mo_2O_7$, SrO were Rietveld fitted as secondary phases. No Sr_2FeMoO_6 impurity was found in this sample. The unit-cell parameters at 300 K ($a = 3.91818(2)$ Å, $c = 12.6691(2)$ Å) are larger than those of Sr_2FeO_4 ($a = 3.864$ Å, $c = 12.397$ Å)[20] but are near those of Sr_2MoO_4 ($a = 3.9168(4)$ Å, $c = 12.859(2)$ Å).[21] This

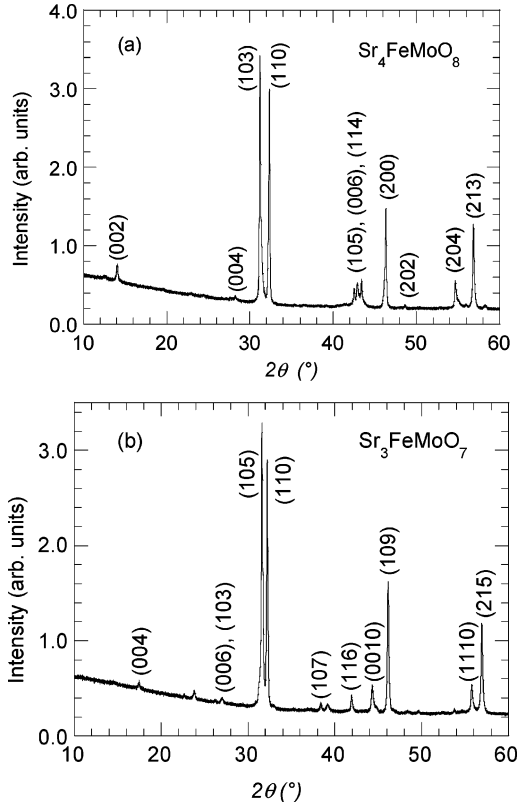

Figure 2. Cu Kα X-ray powder diffraction patterns of (a) Sr_4FeMoO_8 and (b) Sr_3FeMoO_7.

Table 1. Structure Refinement Results for Sr_4FeMoO_8 at 300 and 2 K[a]

atom		300 K	2 K
	a (Å)	3.91818(2)	3.90989(2)
	c (Å)	12.6691(2)	12.6595(2)
	V (Å^3)	194.497(3)	193.529(2)
	R_{wp} (%)	6.20	6.24
	R_p (%)	4.33	4.36
Sr	z	0.35195(9)	0.35174(6)
	U_{iso} (Å^2)	0.004(7)	0.0002(3)
Fe/Mo	U_{iso} (Å^2)	0.004(7)	0.0002(3)
O1	z	0.1599(2)	0.15941(7)
	U_{iso} (Å^2)	0.0096(8)	0.0032(4)
O2	U_{iso} (Å^2)	0.0058(9)	0.0043(4)

[a] Atom positions are Sr (0, 0, *z*), Fe/Mo (0, 0, 0), O1 (0, 0, *z*), O2 (0.5, 0, 0). Isotropic U factors (U_{iso}) were constrained to be equal for the metal atoms.

Table 2. Selected Bond Lengths (Å) of Sr_4FeMoO_8 at 300 and 2 K

	300 K	2 K
Sr1−O1 × 1	2.433(2)	2.435(1)
Sr1−O1 × 4	2.775(1)	2.768(1)
Sr1−O2 × 4	2.712(1)	2.709(1)
Fe/Mo−O1 × 2	2.026(2)	2.019(1)
Fe/Mo−O2 × 4	1.959(1)	1.955(1)

(14) de Gennes, P.-G. *Phys. Rev.* **1960**, *118*, 141.
(15) Prado, F.; Manthiram, A. *J. Solid State Chem.* **2001**, *158*, 307.
(16) Breard, Y.; Michel, C.; Maignan, A.; Raveau, B. *Solid State Commun.* **2001**, *118*, 517.
(17) Battle, P. D.; Bollen, S. K.; Powell, A. V. *J. Solid State Chem.* **1992**, *99*, 267.
(18) Gallon, D. J.; Battle, P. D.; Blundell, S. J.; Burley, J. C.; Coldea, A. I.; Cussen, E. J.; Rosseinsky, M. J.; Steer, C. *Chem. Mater.* **2002**, *14*, 3976.
(19) Larson, A. C.; von Dreele, R. B. *GSAS: General Structure Analysis System*; LANSCE, MS-H805; Los Alamos National Laboratory: Los Alamos, NM, 1994.

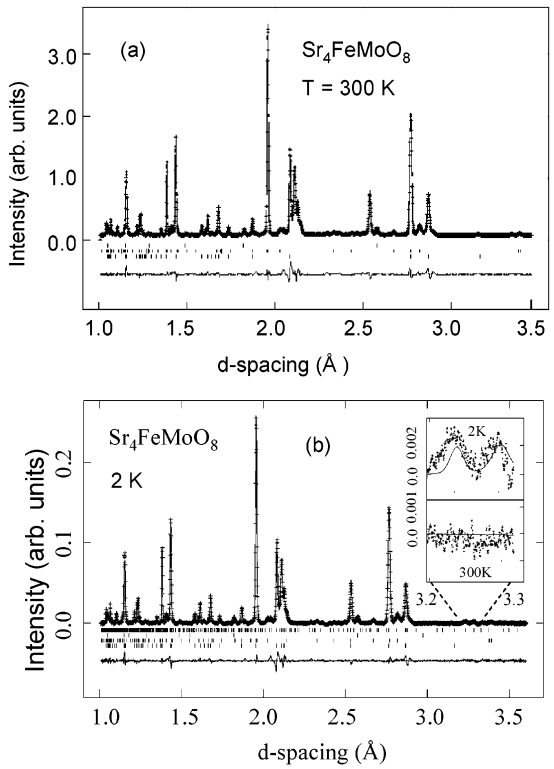

Figure 3. Observed (crosses), calculated (solid lines), and difference neutron powder diffraction profiles of $Sr_4FeMoO_{8\ at}$ (a) 300 K and (b) 2 K. Markers from bottom to top are Sr_4FeMoO_8, $Sr_3Mo_2O_7$, SrO, and Sr_4FeMoO_8 magnetic reflections (2 K). Inset in (b) shows the expanded *d*-spacing range of 3.2 to 3.3 Å, for Sr_4FeMoO_8 at 2 and 300 K, in which the presence of additional magnetic reflections at 2 K is observed.

suggests that the average ionic size[22] of Fe and Mo in Sr_4FeMoO_8 is closer to that of Mo^{4+} (0.65 Å) in Sr_2MoO_4 than that of Fe^{4+} (0.585 Å) in Sr_2FeO_4. Therefore the possible combination of oxidation states for Fe and Mo in Sr_4FeMoO_8 can be Fe^{2+} (0.78 Å)/Mo^{6+} (0.59 Å) or Fe^{3+} (0.645 Å)/Mo^{5+} (0.61 Å) or mixture of both. As expected, the *a* and *c* cell parameters, the unit cell volume (Table 1), and the bond lengths (Table 2) decrease on cooling. There was no evidence of long range ordering of the Fe and Mo cations over the six-coordinate sites. Close inspection of the 2 K neutron diffraction profile for Sr_4FeMoO_8 revealed the presence of two additional reflections at *d* spacings between 3.2 and 3.3 Å, which could be indexed on a magnetic $2a \times b \times 2c$ supercell, ($a = 3.90989(2)$ Å, $c = 12.6595(2)$ Å at 2 K). A magnetic model with antiferromagnetic alignment of adjacent Fe/Mo spins along the *a* and *c* axes and ferromagnetic alignment along the *b* axis was tested and gave a good fit to the magnetic intensities. However, the presence of only two weak magnetic reflections, coupled with the poor counting statistics over this higher *d*-spacing range, precludes an accurate refinement of the direction and size of the magnetic models. A series of possible moments was tried and the best fit to the magnetic peaks (see Figure 3b inset) was obtained with spins parallel to the *b*-axis, and a refined Fe/Mo moment of 3.0(2) μ_B. This is in keeping with an average of ideal Mo^{5+} ($1\mu_B$) and Fe^{3+} ($5\mu_B$) moments.

Table 3. Structure Refinement Results for Sr_3FeMoO_7 at 300 and 2 K[a]

atom		300 K	2 K
	a (Å)	3.94032(5)	3.93129(2)
	c (Å)	20.4671(3)	20.4298(2)
	V (Å^3)	317.775(3)	315.743(3)
	R_{wp} (%)	6.41	7.09
	R_p (%)	4.74	5.25
Sr1	U_{iso} (Å^2)	0.0181(8)	0.0041(7)
Sr2	*z*	0.31441(7)	0.31395(9)
	U_{iso} (Å^2)	0.0144(6)	0.0048(6)
Fe/Mo	*z*	0.10022(8)	0.09931(8)
	U_{iso} (Å^2)	0.0016(3)	0.0012(2)
O1	*z*	0.09563(7)	0.09605(7)
	U_{iso} (Å^2)	0.0025(4)	0.0069(4)
O2	*z*	0.1973(1)	0.19644(1)
	U_{iso} (Å^2)	0.0106(9)	0.0126(6)
O3	U_{iso} (Å^2)	0.011(2)	0.022(1)

[a] Atom positions are Sr1 (0, 0, 0.5), Sr2 (0, 0, z_1), Fe/Mo (0, 0, z_2), O1 (0, 0.5, z_3), O2 (0, 0, z_4), O3 (0, 0, 0).

Table 4. Selected Bond Lengths (Å) of Sr_3FeMoO_7 at 300 and 2 K

	300 K	2 K
Sr1−O1 × 8	2.781(1)	2.777(1)
Sr1−O3 × 4	2.786(1)	2.780(1)
Sr2−O1 × 4	2.697(2)	2.692(2)
Sr2−O2 × 1	2.398(2)	2.401(3)
Sr2−O2 × 4	2.797(1)	2.788(1)
Fe/Mo−O1 × 4	1.973(1)	1.967(1)
Fe/Mo−O2 × 1	1.986(2)	1.984(3)
Fe/Mo−O3 × 1	2.052(2)	2.029(2)

Neutron diffraction data for Sr_3FeMoO_7 were also Rietveld fitted in space group *I*4/*mmm*. The resulting structural parameters and atomic coordinates are given in Table 3 and the corresponding bond lengths are listed in Table 4. The observed and calculated diffraction profiles are plotted in Figure 4. A small impurity phase (<2 wt %) of Sr_3MoO_6 was also identified in the neutron diffraction pattern. The unit cell parameters ($a = 3.94032(5)$ Å, $c = 20.4671(3)$ Å) for Sr_3FeMoO_7 are larger than those of $Sr_3Fe_2O_7$ ($a = 3.8424(1)$ Å, $c = 20.1148(2)$ Å)[23] but are smaller than those of $Sr_3Mo_2O_7$ ($a = 3.967(1)$ Å, $c = 20.588(5)$ Å).[24] This again suggests a mixed oxidation state of Fe^{3+}/Fe^{2+} for Fe and corresponding Mo^{5+}/Mo^{6+} for Mo in this material. Both the *a* and *c* cell parameters and bond lengths decrease on cooling. As in the case of Sr_4FeMoO_8, there was no evidence of long range ordering of the Fe and Mo cations. Study of the 2 K diffraction profile of Sr_3FeMoO_7 revealed no additional reflections, or significant changes in peak intensities in comparison to the room-temperature pattern, and the data were again well-fitted by a model, tetragonal space group *I*4/*mmm*, consisting of nuclear scattering only.

Magnetization Measurements. No clear magnetic transition is observed in the susceptibility data of Sr_4FeMoO_8 (Figure 5). However, the field dependence of the magnetization of Sr_4FeMoO_8 is hysteretic (Figure 6) with a coercivity of 800 Oe. The small saturated moment ~0.2 μ_B, coupled with the apparent antiferromagnetism in the neutron scat-

(20) Dann, S. E.; Weller, M. T.; Currie, D. B. *J. Solid State Chem.* **1991**, *92*, 237.
(21) Shirakawa, N.; Ikeda, S.-I.; Matsuhata, H.; Bando, H. *Jpn. J. Appl. Phys.* **2001**, *40*, L741.
(22) Shanon, D. *Acta Crystallogr*. **1976**, *32*, 751.
(23) Dann, S. E.; Weller, M. T.; Currie, D. B.; Thomas, M. F.; Al Rawwas, A. D. *J. Mater. Chem*. **1993**, *3*, 1231.
(24) Steiner, U.; Reichelt, W. *Z. Naturforsch. B* **1998**, *53*, 110.

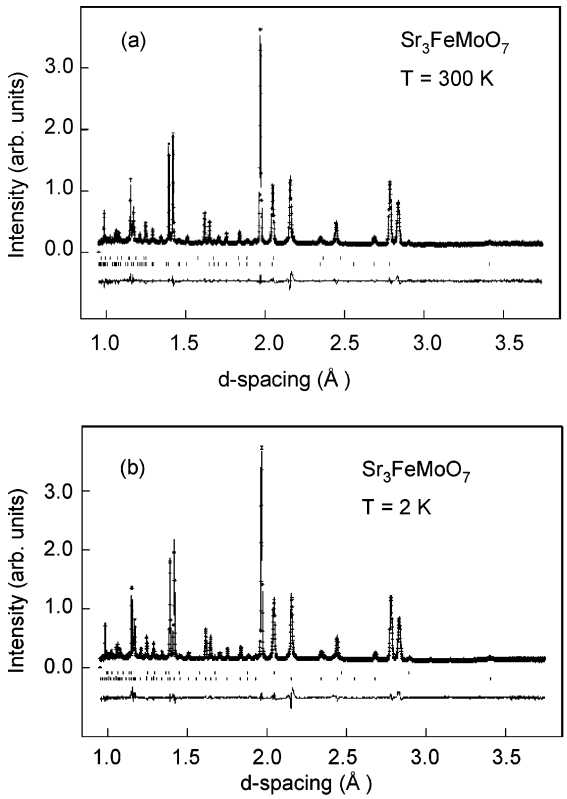

Figure 4. Observed (crosses), calculated (solid lines), and difference neutron powder diffraction profiles of $Sr_3FeMoO_{7\ at}$ (a) 300 K and (b) 2 K. Markers from bottom to top are Sr_3FeMoO_7 and Sr_3MoO_6.

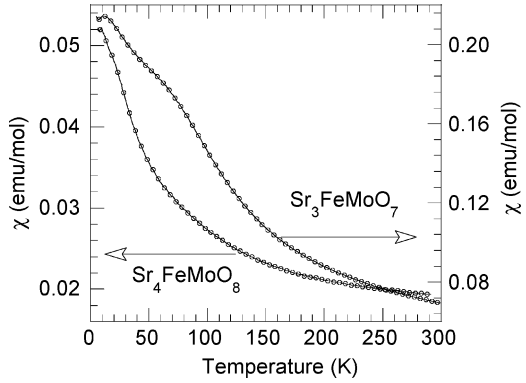

Figure 5. Molar magnetic susceptibilities of Sr_4FeMoO_8 and Sr_3FeMoO_7 as a function of temperature.

tering suggests that Sr_4FeMoO_8 is a weak ferromagnet (canted antiferromagnet).

The magnetic susceptibility of Sr_3FeMoO_7 (Figure 5) sharply increases below ∼200 K, characteristic of a ferromagnetic interaction. However, neutron diffraction data collected at 2 K show no evidence of magnetic Bragg scattering, suggesting that there is no coherent long-range magnetic ordering in this material and therefore that Sr_3FeMoO_7 is a spin-glass at low temperatures. The susceptibility anomaly at ∼60 K may correspond to the spin freezing transition. The field dependence of the magnetization of Sr_3FeMoO_7 (Figure 6) is again hysteretic with a coercive field of 1030 Oe and a saturated moment of ∼0.8 μ_B. The coercivities of both these novel RP analogues are much higher than that observed in Sr_2FeMoO_6 (all reported values <100 Oe), reflecting the greater anisotropy of these layered systems.

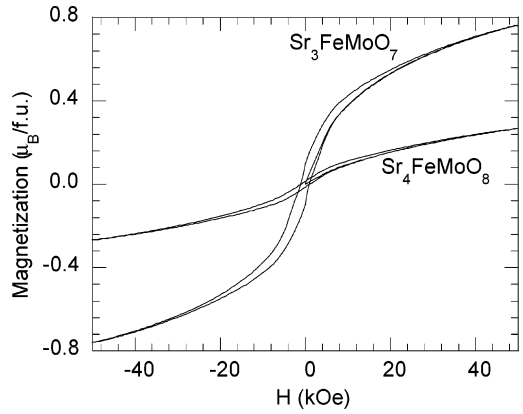

Figure 6. Magnetization-field hysteresis loops of Sr_4FeMoO_8 and Sr_3FeMoO_7 at 5 K.

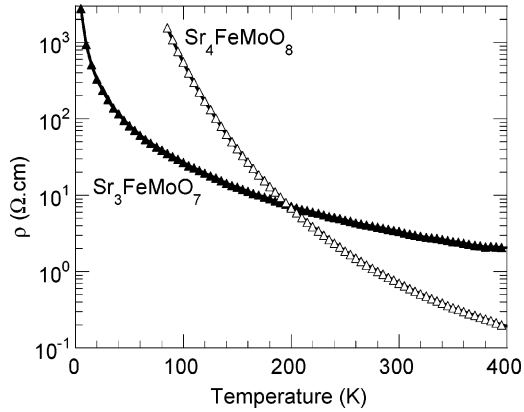

Figure 7. Resistivities of Sr_4FeMoO_8 and Sr_3FeMoO_7 as a function of temperature.

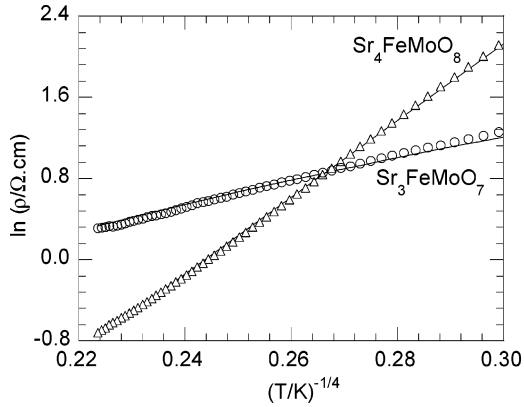

Figure 8. Plots for Sr_4FeMoO_8 and Sr_3FeMoO_7 showing fits of the resistivity data to a VRH model in the temperature range of 150−400 K.

Electronic Transport Properties. The temperature dependences of electrical resistivity for Sr_4FeMoO_8 and Sr_3FeMoO_7 are shown in Figure 7. The temperature coefficient of resistivity is negative throughout ($d\rho/dT < 0$), showing that both materials are semiconducting. The room-temperature resistivities of Sr_4FeMoO_8 and Sr_3FeMoO_7 are 0.71 and 3.34 Ω·cm, respectively. The resistivity of Sr_4FeMoO_8 was too large to be measured accurately below 85 K.

To understand the transport mechanism in these compounds, the resistivity data were fitted according to a thermally activated model, $\rho(T) = \rho_0 \exp(E_0/kT)$, and a variable range hopping (VRH) model,[25] $\rho(T) = \rho_0 \exp(T_0/T)^{0.25}$, in the temperature range of 150 to 400 K. Band gaps

for the two materials were estimated from a thermally activated model fit to the data, which yielded values of 125 and 46 meV for Sr_4FeMoO_8 and Sr_3FeMoO_7, respectively. However, the VRH model gave a better fit to the data for both samples (Figure 8). The obtained values of T_0 from the VRH model are 2.05×10^6 and 4.66×10^3 K for Sr_4FeMoO_8 and Sr_3FeMoO_7, respectively. In the VRH model, the parameter T_0 is related to inverse localization length, α, by the expression, $kT_0 = 18\alpha^3/3N(E_F)$, where $N(E_F)$ is the density of states at the Fermi energy. The larger value of T_0 for Sr_4FeMoO_8, and hence the smaller localization length, suggests that the carriers are more localized in Sr_4FeMoO_8, which is more two-dimensional than Sr_3FeMoO_7.

There was no change in resistivity of either sample in the applied fields of up to 50 kOe over the whole temperature range, and hence no MR effect was observed in either of the samples.

(25) Mott, N. F. *Metal−Insulator Transitions*, 2nd ed.; Taylor & Francis: London, 1990.

Conclusions

We have synthesized two new SFMO analogue Ruddlesden−Popper phases: Sr_3FeMoO_7 and Sr_4FeMoO_8. No long-range magnetic order is observed in Sr_3FeMoO_7, although a spin-glassy ferro- or ferrimagnetism is observed at low temperatures. Two weak magnetic Bragg reflections were observed for Sr_4FeMoO_8 at 2 K and are fitted by $2a \times b \times 2c$ antiferromagnetic model. However, local Fe/Mo order results in a small bulk magnetization. Resistivity measurements have shown a semiconducting behavior in both materials, with no MR effect in applied fields of up to 50 kOe and over the temperature range of 5 to 400 K. A variable range hopping model fits well to the resistivity data above 150 K in both materials.

Acknowledgment. We thank the Ministry of Science and Technology, Government of Pakistan, and EPSRC (grant GR/R30518) for funding, and Dr. R. Ibberson for assistance with neutron data collection.

CM0479178